

Electromagnetic and Thermal Analysis Using Finite Element Method of Axial Flux BLDC Motor

H. Suryoatmojo, R. Mardiyanto, D.C. Riawan, M. Ashari, S. Anam, E. Setijadi and Dwi Haryanto
Department of Electrical Engineering, Institut Teknologi Sepuluh Nopember (ITS),
Surabaya, Indonesia

Abstract: The development of electric vehicle research on the design of an optimized, efficient and reliable motor drive is required to improve the performance of the electric vehicle. The design of compact motor drive with high power to weight ratio is required in the application of motor drive for electric vehicle. In this research, electromagnetic-thermal analysis of DC axial flux brushless motor is performed. In this experiment, the motor is designed to produce an output power of 12 kW. Electromagnetic analysis that performed in this research including electrical parameters, field characteristics and core losses on the motor. The analysis is done using finite element method. The design results obtained are axial flux brushless DC motor with size 220 cm using 12 stator slot and 10 pole rotor. Produces 12.36 kW of output power, 2,388 rpm of speed, 392 W of core loss and 49.4 Nm of torque. This motor has a voltage rating of 400 V DC and 29.2 A of the input current. Produces 12.36 kW of output power, 2,388 rpm of speed, 392 W of core loss and 49.4 Nm of torque. The voltage rating of motor is 400 V DC and the input current is 29.2 A. The convection heat transfer coefficient of the motor is 51.7 W/m² °C and the maximum heat that occurs in the motor is 73.037°C.

Key words: Axial flux BLDC motor, finite element analysis, electromagnetic-thermal analysis, convection heat transfer, power, design

INTRODUCTION

In the face of the increasing need for electric vehicles, many companies, educational institutions and government agencies participate in the research, development and production of electric vehicles. But today, electric vehicles are not very competitive when compared to conventional fuel vehicles. This is due to the limitations of electric vehicles such as reach, poor acceleration and expensive production costs. Motor drive technology is an important factor that can affect the range and performance of electric vehicles. Some criteria such as cost, reliability, efficiency, maintenance, durability, weight, size and noise level are the main considerations in choosing electric motor drive system on electric vehicles (Yang *et al.*, 2004). In addition, developments in the technology side of batteries and inverter technology are growing, making electric car technology increasingly in demand (Bambang *et al.*, 2010).

One of the developments of motor drive design which is widely used in research of electric vehicle is the use of Induction Motor (IM) and permanent magnet Brushless DC Motor (BLDCM). A study by Chang (1994) concluded

in his survey, that neither the Induction Motor (IM) nor the permanent magnet Brushless DC (BLDC) motor was either used as an electric vehicle propulsion. Several permanent-magnet motors have been developed for electric vehicle applications due to their advantages, such as high power density requirements, high efficiency, high initial torque and high cruising speed. In motor driving classes for electric vehicles, Axial Flux (AF) is competing with radial flux with several advantages in terms of load capability, heat dissipation, air gap and the use of rotor back iron (Vansompel, 2013). An Axial Flux (AF) motor has a size and weight of a smaller/compact motor when compared to a radial flux motor in the same power capacity. Thus, the Axial Flux Brushless DC (AFBLDC) motor is suitable for applied to electric vehicles where the weight and size of the motor as the main driver of electric vehicles can be overcome (Vansompel, 2013).

At this time, axial flux brushless DC motors are widely used, so, motors are required to have high power densities. This can cause the motor to have a large electromagnetic load and will increase the heat as well. So, the problem of thermal design on a motor is an important thing to be made a research (Xiaowei and Tiecai, 2011). Therefore, electromagnetic and thermal

(Coupled electromagnetic-thermal) analysis is required to be able to calculate the condition of a machine in actual operation at the design stage (Marignetti *et al.*, 2008).

This time, axial flux brushless DC motor more used, so, motor are required to has high power densities. It can be effect motor have large electromagnetic load and will making heat increase. So, the problem of terminal design on the motor is an important to be the research (Xiaowei and Tiecai, 2011). Therefore, electromagnetic analysis and thermal (coupled electromagnetic-thermal) needed to be able calculate condition a machine in actual operation at design stage (Marignetti *et al.*, 2008). This research describes a 3-D electromagnetic and thermal analysis of axial flux motor DC. The motor design analyzed in this research uses a single-sided Axial Flux (AF) BLDC design. In this study, the analyzes performed include the electromagnetic loss analysis that occurs on the BLDC axial flux motor and resulting heat generated by the motor. The analysis of this research is based on finite-element by using software capable of analyzing the motor according to the method. It is hoped that through this analysis, we can illustrate the electromagnetic losses that can occur in the BLDC axial flux motors and their effect on the heat that occurs on the motor. So that, the maximum utilization of the motor and become a reference in the development of electric vehicle technology in the future.

MATERIALS AND METHODS

Parameters of axial flux BLDC motor: BLDC motor is one type of DC motor that has a permanent magnet in the rotor and anchor coil on the stator. There are two types of BLDC motors when viewed in terms of flux flow direction, radial flux BLDC and axial flux BLDC. The structure of the proposed BLDC motor is single rotor with single stator. Such type of this machine has very high ratio in weight to its power. Figure 1 shows the construction of the proposed BLDC motor. The BLDC motor used is a motor with a power output of 12 kW with a speed of 2,388 rpm. Since, the motor structure is symmetrical, it is sufficient to consider only half of the motor geometric model used in the motor analysis. The main size of the BLDC motor will be shown in Table 1.

Electromagnetic analysis

Calculation of core loss: Losses that occur in the motor is the main source that causes heat on the motor. The losses incurred are core losses, ohmic losses and mechanical losses. The core losses and ohmic losses account for more than 90% of the total losses incurred on the motor. The amount of iron core losses that occur depends on the selection of materials that will be

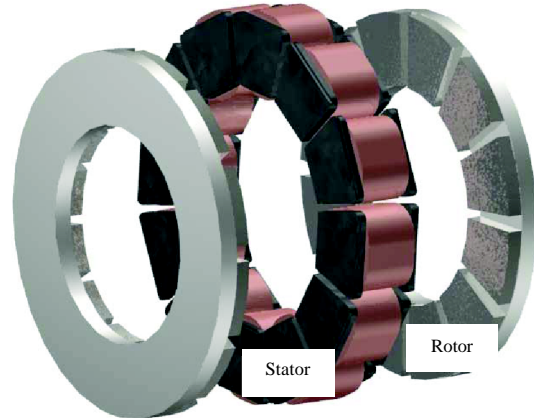


Fig. 1: Construction of axial flux BLDC motor
(<https://impremedia.net/axial-flux-motor>)

Table 1: Stator and rotor data

Size	Length (mm)
Stator length	20
Stator outer diameter	220
Stator inner diameter	104.5
Rotor outer diameter	220
Rotor inner diameter	104.5

used on the motor. Material type used in this research is M800-50A. The iron core loss can be expressed as:

$$P_v = P_c + P_h + P_e \quad (1)$$

$$= K_c (fB_m)^2 + K_h f B_m^2 + K_e (fB_m)^{1.5} \quad (2)$$

$$= K_1 B_m^2 + K_2 B_m^{1.5} \quad (3)$$

Where:

$$K_1 = K_h f + K_c f^2 \quad (4)$$

$$K_2 = K_e f^2 \quad (5)$$

With K_c , K_h and K_e are the eddy current loss coefficients, hysteresis losses and excess loss or additional losses incurred on the motor. While P_v , P_h , P_c and P_e are iron core losses, hysteresis losses, eddy current losses and excessive losses respectively. Meanwhile, the classic eddy current coefficients, K_c can be calculated by the Eq 6:

$$K_c = \pi^2 \cdot \sigma \cdot \frac{d^2}{6} \quad (6)$$

Where:

• = The conductivity

d = The thickness of the sheet of one laminate

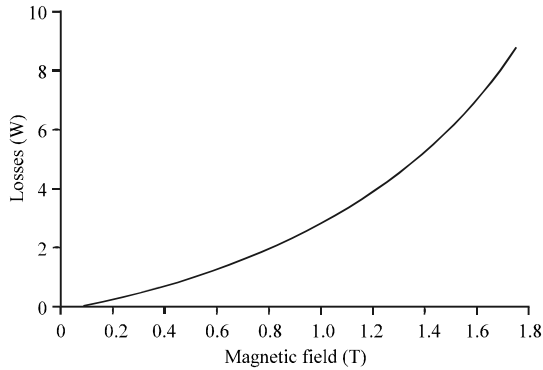


Fig. 2: Material B-P M800-50A on 50Hz curve

To get the value of K1 and K2, minimization must be done to the squared form as follows:

$$f(K1, K2) = \sum [P_{vi} - (K1B_{mi}^2 + K2B_{mi}^{1.5})]^2 = \min \quad (7)$$

where, P_{vi} , B_{mi} is the i -th point of the data measured on the material loss curve of the material. While the other two-loss coefficients, K_e and K_h can be determined from the following equation:

$$K_h = \frac{(K1 - K_{cfo}^2)}{f_o} \quad (8)$$

$$K_e = \frac{K2}{f_o^{1.5}} \quad (9)$$

where, f_o is frequency of test used material losses curve. Material used silicon iron M800-50 with losses curve on the type on frequency 50 Hz will be shown on Fig. 2.

Calculated of ohmic loss: The ohmic losses consist of I^2R losses and eddy current losses. The magnitude of the copper loss depends on the current density, material conductivity and current density distribution of the conductor. The ohmic losses occur when the motor is rotating. The current passing through the resistance of the stator winding will result in losses. In a conductive time and when the eddy current loss is not considered, the density of the windings/copper loss can be expressed as:

$$P_{cu} = \frac{(J \cdot J^*)}{2\sigma} \quad (10)$$

Where:

J = The current density

J^* = The conjugate complex of the current density

Thermal analysis: Electromagnetic losses in the stator will affect heat on the motor when it is spinning. Rotation of the rotor when the motor is working will cause airflow on the air gap. So, the heat transfer that occurs in the motor should consider the rotation of the rotor. The dominant heat transfer mechanisms occurring in this type of machine tend to be convective and conductive, although heat transfer in the form of radiation also needs to be taken into account in the thermal modeling of a machine. Convection heat transfer data is usually non-dimensional, so, the number of variables in the problem is reduced and the result can be applied generally to various engine sizes. The most relevant non-dimensional group here is Reynolds Re 's number which summarizes the rotor speed and engine size; Nu Nusselt's average number is a non-dimensional convective heat transfer coefficient; C_w represents non-dimensional air mass flow rate through the machine; and geometric parameters such as Gap ratio G . In a disc machine or usually called an axial flux machine, the equation for calculating the heat transfer coefficient of convection can be explained as follows:

$$Nu = \frac{hR}{k} \quad (11)$$

$$Nu = A Re^\theta \quad (12)$$

$$Re^\theta = \frac{\omega R^2}{\nu} \quad (13)$$

$$G = \frac{g}{R} \quad (14)$$

Where:

Nu = Nusselt numbers

Re^θ = Reynold number of rotation

ω = Speed (rad/sec)

ν = The kinematic viscosity of the fluid

k = Fluid conductivity

R = Rotor diameter in meters

G = Gap ratio

g = The air gap width between the stator and the rotor (m)

The kinematic data of viscosity in various temperature conditions are explained in Table 2. Here, it is assumed that ambient temperature is 25°C, the air conductivity is 0.024. Then, the kinematic viscosity data of fluid from Table 3 and motor data used for calculation of heat transfer coefficient of convection can be determined as follows:

Table 2: Kinematic viscosity data in various temperature conditions

Temperature (°C)	Kinematic viscosity×10 ⁻⁵ (m ² /sec)
0	1.33
20	1.51
40	1.69
60	1.89
80	2.09

Table 3: The average correlation of turbulent heat transfer

G	A	B
0.0106	0.0790	0.640
0.0127	0.0888	0.633
0.0170	0.0406	0.682
0.0212	0.0315	0.691
0.0297	0.0347	0.679
0.0467	0.0234	0.712

- Rotor diameter = 220 mm = 0.22 m
- Speed = 220 rpm = 250 rad/sec
- Air gap = 1 mm = 0.001 m
- Air conductivity = 0.024 W/m°C (at 25°C)
- Kinematic air viscosity = 1.51e⁻⁵ (m²/sec)

Then, we can calculate:

$$Re\theta = \frac{250 \cdot 0.22^2}{1.51 \cdot 10^{-5}} = 8.01 \cdot 10^5$$

$$G = \frac{0.001}{0.22} = 0.045, G \approx 0.01$$

Howey *et al.* (2011) states that the transition from the laminar stream to the turbulent laminar is seen from Reynolds $Re > 3e5$. In the construction of the selected motor has a Reynolds number of 8.01×10^5 . It is stated that the air flow in the motor is turbulent flow. Based on (Howey *et al.*, 2012), the average correlation of turbulent heat transfer shown in Table 3.

From Table 3, it can be seen that the value of A and B for $G \approx 0.1$ 0.079 and 0.640 are respectively. So, the Nusselt number can be calculated as follow:

$$Nu = A Re\theta^B = 0.0790 \times 8.01 \times 10^{5 \cdot 0.640} = 474.2$$

So, the heat transfer coefficient can be obtained:

$$= \frac{474.2 \times 0.024}{0.22}$$

$$= 51.7 \frac{W}{m^2}$$

RESULTS AND DISCUSSION

Electrical parameters of axial flux BLDC motor: From previous research in designing of BLDC motor with finite element-based software, all electrical parameters such as input current, rated voltage, rated torque and power factor

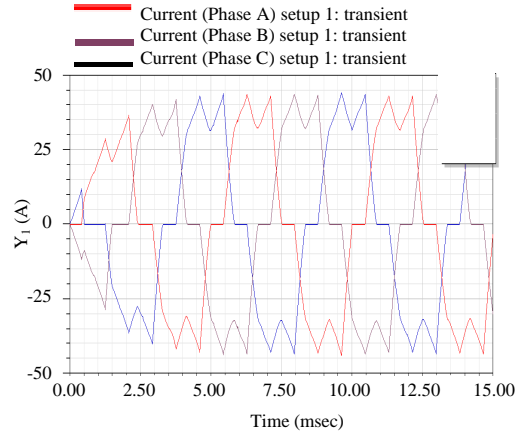


Fig. 3: Current waveform for t = 15 msec

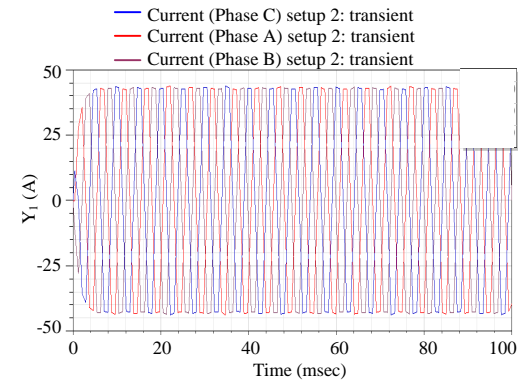


Fig. 4: Current waveform for t = 100 msec

of motor are tested in this simulation (Suryatmojo *et al.*, 2017). The input current and voltage values are influenced by the incoming source of the control circuit with a 400 V DC source. The current to the motor depends on the number of winding. This model is simulated in two different time intervals: 15 and 100 msec, each interval is simulated with different sampling frequency. In steady state simulation with duration 2.5 msec, BLDC motor draws current about 29.2 A. Figure 3 and 4 explain the current waveforms at two different time intervals.

From the simulation, it can be seen that the voltage value at the stator is 183.3 V. Here, the appeared voltage at the stator side represents the output voltage from the inverter. Figure 5 and 6 show voltage waveforms at two different time intervals. From this Fig. 6, it can be seen that steady state condition from the stator voltage is 2.5 msec. In order to perform effectiveness of the design, in this simulation BLDC motor is tested with several speed reference. For example, BLDC motor is set with speed reference in 2388 rpm and it generates average induced torque 49,44 Nm. Figure 7 shows the output torque of BLDC motor per minutes.

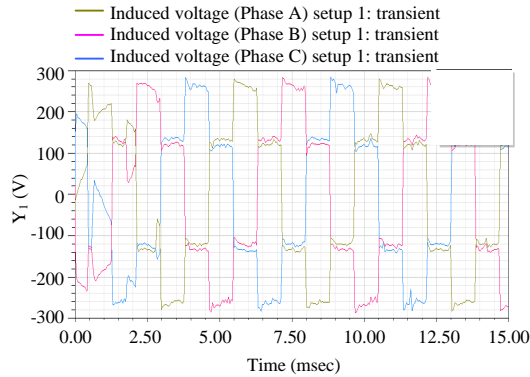


Fig. 5: Voltage waveform for t = 12.5 msec

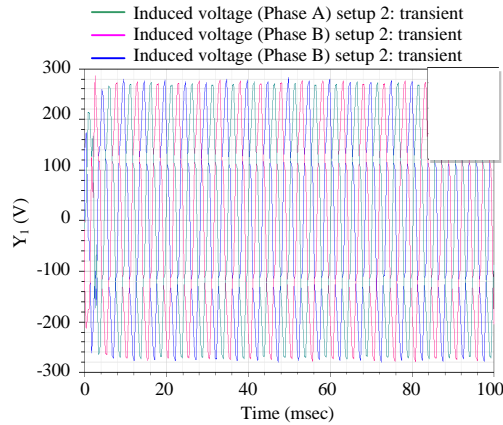


Fig. 6: Voltage waveform for t = 100 msec

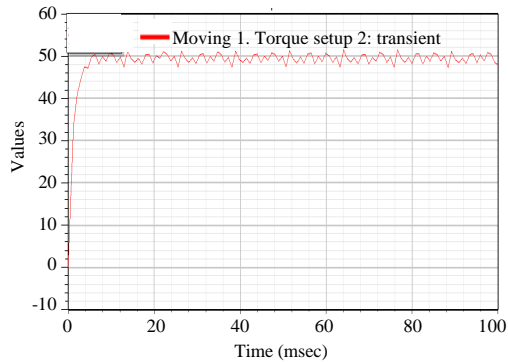


Fig. 7: Torque output for t = 100 msec

For several speed references the value of induced torque will change significantly. The torque characteristics of BLDC axial flux motor speed will be shown in Fig. 8. From this figure it can be seen that if speed of the BLDC motor increases then the torque is gradually decreases.

Next electrical parameter to be performed is the value of power factor ($\cos \phi$). Here, the definition of $\cos \phi$ is the

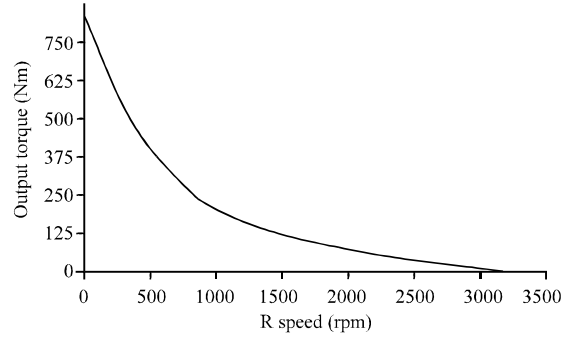


Fig. 8: Speed torque characteristic (Output torque setup 1: performance)

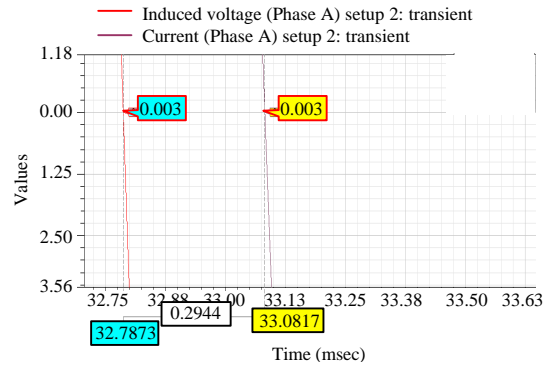


Fig. 9: Time differences when V = 0 and I = 0 msec

difference of phase angle between voltage wave and current wave of BLDC motor. The value of $\cos \phi$ can be calculated as follows:

$$\alpha = \frac{t_{(I=0)} - t_{(V=0)}}{T} \times 360^\circ$$

To simplify the above equation, Fig. 9 and 10 explain the mechanism to find ϕ . The value of $\cos \phi$ can be determined by comparing time between current and voltage. At the zero axis, cross section of current and voltage waveform indicate the displacement angle of current and voltage. Then, it can be used for determining the value of ϕ . From the simulation, total period of time to finish full waveform is = 5.0251 msec and displacement of time between current and voltage is 0.294, then the value of ϕ can be calculated become:

$$\alpha = \frac{0.294}{5.0251} \times 360^\circ = 21^\circ$$

From the equation, the value of ϕ in degree is 21° . Then, this value can be converted to power factor become

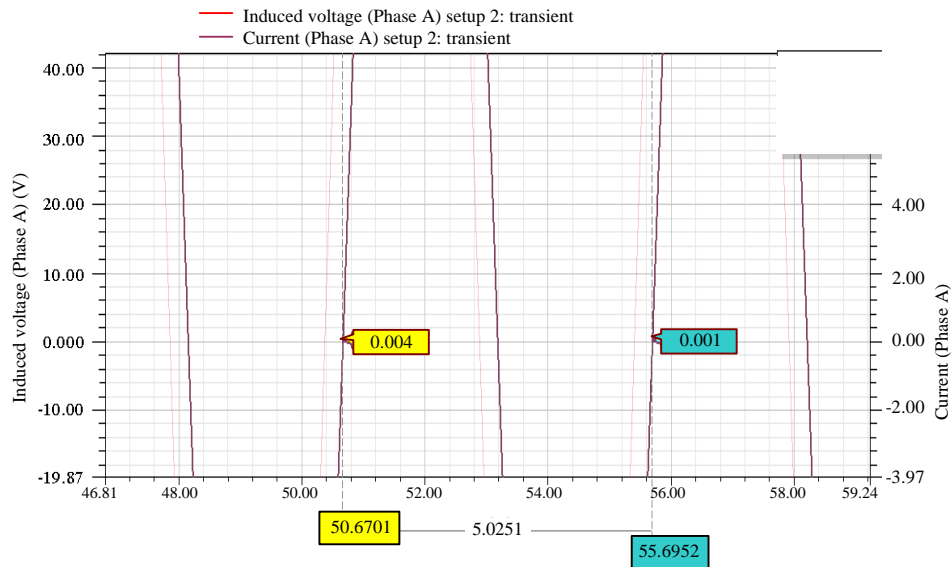


Fig. 10: Total time period for full wave

$\cos 21^\circ = 0.93$. From simulation it can be observed that input current of the motor is 29.2 A and the input voltage is 183.3 V. Then, The electrical power consumes by this motor is:

$$\begin{aligned} P_{in} &= 3 \cdot V \cdot I \cdot \cos \alpha \\ &= 3,174.5 \times 29.2 \times 0.93 \\ &= 14.93 \text{ kW} \end{aligned}$$

Meanwhile, the output power of this motor depends on the speed of the motor and its torque. From simulation the torque is 49,44 Nm and motor speed is 2,388 rpm. Therefore, the output power becomes:

$$\begin{aligned} P_{out} &= T \cdot \omega \text{ and } \omega = \frac{2 \cdot \pi \cdot n}{60} \\ &= \frac{2 \times 3.14 \times 2,388}{60} \\ &= 250 \frac{\text{rad}}{\text{sec}} \\ P_{out} &= 49.44 \times 250 \\ &= 12.36 \text{ kW} \end{aligned}$$

Characteristics of field and core loss on the stator: From the simulation with data acquisitions for 0.1 sec, we got the flux distribution map in the stator. A relatively high value of flux is found in the slot and tooth where there is winding where the field is generated. Figure 11 shows the field characteristics occurring in the stator.

The core losses are affected by two things, namely hysteresis loss and eddy current loss arising at the

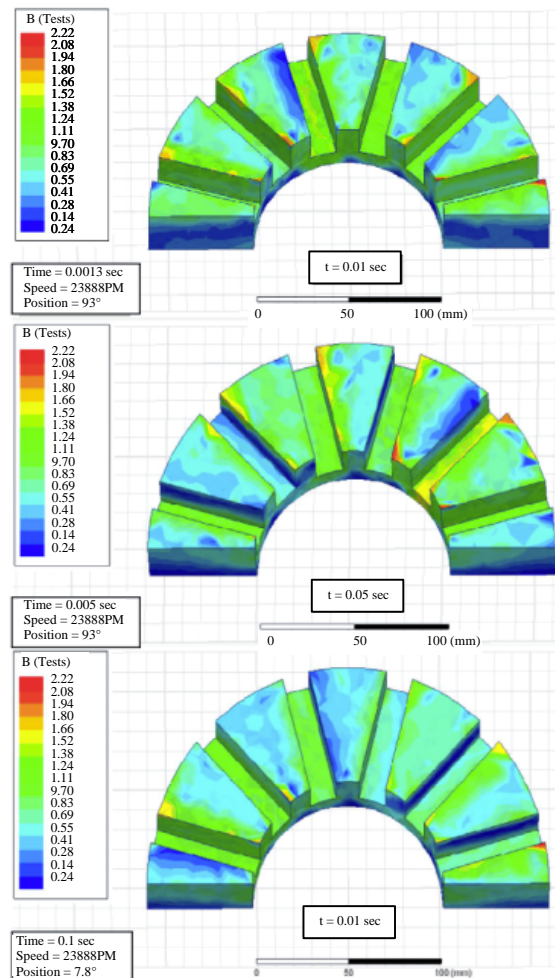


Fig. 11: Characteristics of stator field

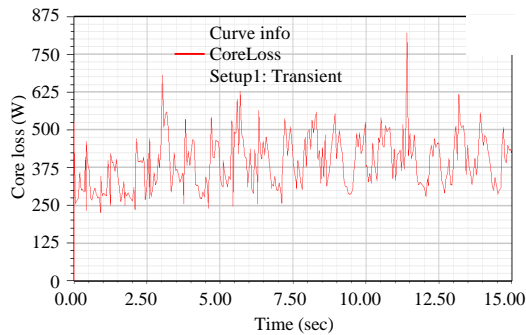


Fig. 12: The magnitude of core losses in the stator

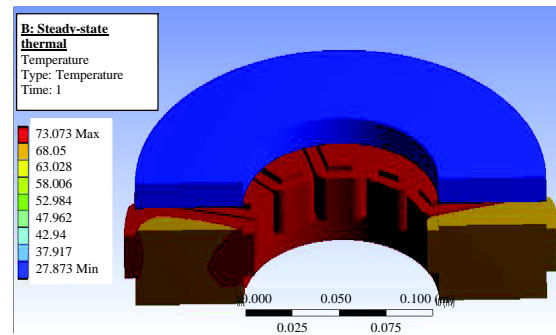


Fig. 14: Heat on the motor AFBLDC

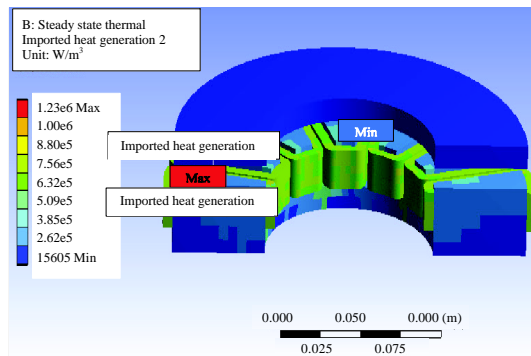


Fig. 13: Imported heat generation in steady-state thermal analysis

stator core. Where core losses depend on the flux value, especially, the maximum flux arising on the stator core. Figure 11 shows the stator field characteristics and the maximum flux value arising on the stator is 2.4 Tesla, at $t = 0.1$ sec. Figure 10 shows the magnitude of core losses occurring on the BLDC axial flux motor.

In simulations with 3-D analysis software as shown in Fig. 12 shows the core loss values at each change of time. And from the picture above also can know the average value of core loss generated on motor is equal to 392 W.

Results of electromagnetic-thermal simulation of axial flux BLDC motor: The heat source that arises on the motor is the electromagnetic losses occurring on the motor, on the steady-state thermal analysis can be seen the distribution of electromagnetic losses that occur as shown in Fig. 13. From the Fig. 11 can be seen that the heat generation, is an electromagnetic load that causes heat on the motor. The maximum value contained in the stator and winding is 1.1264×10^6 W/m³ while the smallest value is at the rotor of 15,605 W/m³. After the heat generation is imported, the convective heat transfer coefficient can be determined by the Eq. 11:

In the formula, the magnitude of convection heat transfer coefficient (h) is influenced by the value of the Nusselt (Nu) number, the diameter of the rotor and the fluid conductivity (wherein the air gap of the fluid used air) is present on the motor. With this formula, we get the value of convection heat transfer coefficient of $51.7 \text{ W/m}^2 \text{ } ^\circ\text{C}$. With the formula, we get the value of convection heat transfer coefficient of $51.7 \text{ W/m}^2 \text{ } ^\circ\text{C}$. The greater the value of heat transfer coefficient, the lower the resulting temperature rise. Conversely, if the smaller the resulting temperature rise, the coefficient value will be higher.

From Fig. 14, it can be seen that the temperature on the stator is higher than the temperature on the rotor. Assuming a room temperature of 25°C , we obtained the maximum temperature at the stator of 73.037°C and the minimum temperature on the rotor is 27.837°C . The temperature at the stator is higher due to the winding which is the excitation place. While the temperature at the rotor is lower due to no excitation, it is replaced by permanent magnets and rotor in a rotating condition.

CONCLUSION

From simulation results of axial flux BLDC motor with 12 kW with the speed of 2,388 rpm, BLDC motor requires current 29.2 A, output voltage 183.3 V, power factor 0.9, input power 14.93 kW output power 12.36 kW and torque is 49.4 Nm. Due to it is not operated near to optimum speed and torque, proposed design of Axial Flux BLDC motor have the efficiency approximately 82.7%. Not only electrical parameters, this model also able to perform thermal condition in the core of the BLDC motor. Based on the motor construction, the convection heat transfer coefficient of this motor is $51.7 \text{ W/m}^2 \text{ } ^\circ\text{C}$. Meanwhile, the maximum heat on the motor is 73.073°C at the stator and minimum 27.873°C at the rotor side.

REFERENCES

- Bambang, S., M. Ashari and M.H. Purnomo, 2010. Universal algorithm control for asymmetric cascaded multilevel inverter. *Int. J. Comput. Appl.*, 10: 38-44.
- Chang, L., 1994. Comparison of ac drives for electric vehicles-A report on experts opinion survey. *IEEE. Aerosp. Electron. Syst. Mag.*, 9: 7-11.
- Howey, D.A., A.S. Holmes and K.R. Pullen, 2011. Measurement and CFD prediction of heat transfer in air-cooled disc-type electrical machines. *IEEE. Trans. Ind. Appl.*, 47: 1716-1723.
- Howey, D.A., P.R. Childs and A.S. Holmes, 2012. Air-gap convection in rotating electrical machines. *IEEE. Trans. Ind. Electron.*, 59: 1367-1375.
- Marignetti, F., V.D. Colli and Y. Coia, 2008. Design of axial flux PM synchronous machines through 3-D coupled electromagnetic thermal and fluid-dynamical finite-element analysis. *IEEE. Trans. Ind. Electron.*, 55: 3591-3601.
- Suryoatmojo, H., R. Mardiyanto, G.B.A. Janardana and M. Ashari, 2017. Design of axial flux brushless DC motor based on 3D finite element method for unmanned electric vehicle applications. *J. Theor. Appl. Inf. Technol.*, 95: 1034-1040.
- Vansompel, H., 2013. Design of an energy efficient axial flux permanent magnet machine. Ph.D Thesis, Ghent University, Ghent, Belgium.
- Xiaowei, W. and L. Tiecai, 2011. A 3-D electromagnetic thermal coupled analysis of permanent magnet brushless DC motor. *Proceedings of the 1st International Conference on Instrumentation, Measurement, Computer, Communication and Control*, October 21-23, 2011, IEEE, Beijing, China, ISBN:978-0-7695-4519-6, pp: 15-18.
- Yang, Y.P., Y.P. Luh and C.H. Cheung, 2004. Design and control of axial-flux brushless DC wheel motors for electric vehicles-part I: Multiobjective optimal design and analysis. *IEEE. Trans. Magn.*, 40: 1873-1882.